8
Quantum Correlations in Neutrino Oscillations in Curved Spacetime

This chapter is based on the Ref. [98]. Following the motivation for the study of the nature of correlations embedded in the neutrino-system under different circumstances, in this chapter, we explore various spatial quantum correlations in neutrinos propagating and oscillating in curved spacetimes. A model describing neutrino-antineutrino oscillations due to gravitational Zeeman splitting [83] has been considered to incorporate the effect of curved spacetime around a massive object following Kerr geometry. Specific choice of Kerr geometry that has also been justified in Ref. [223, 224] causes the neutrino-antineutrino asymmetry (apart from early Universe processes) in the present era when the Universe has cooled down and it can happen when the neutrino propagates through a spacetime curvature produced by e.g., a rotating black-hole, *i.e.,* Kerr geometry. Basically, when fermions propagate in curved spacetime, it generates gravitational interaction due to coupling of its spin with spacetime curvature connection. This gravitational interaction appears as a CPT violating term generating opposite signs (and hence asymmetry) between left handed and right handed partners of the fermion under CPT transformation. Specifically for neutrinos, this property can generate neutrino-antineutrino asymmetry. This interaction for neutrinos appears to be non-zero if the background metric is of the rotating black hole, *i.e.,* Kerr geometry. Hence, it is interesting to analyze correlation aspects of neutrinos in such spacetime geometry due to its compelling physical implications.

We have considered one and two-flavour neutrino scenarios, which lead to two- and four-level systems of neutrino-antineutrino oscillation, respectively. To study the correlation measures, the idea of mode entanglement is used [15], as discussed ahead in this chapter.

The plan of this chapter is as follows. In section 8.1 we briefly review the gravitational Zeeman effect. Then we discuss the nature of quantum correlations in gravity induced neutrino-antineutrino oscillations for one and two-flavour scenarios in section 8.2.

8.1 Gravitational "Zeeman effect"

The general form of invariant coupling of a spin-1/2 particle with spacetime curvature is described by the following Lagrangian [225–232]

$$\mathcal{L} = \sqrt{-g}\left(\frac{i}{2}\bar{\Psi}\gamma_a\overset{\leftrightarrow}{\mathcal{D}}_a\Psi - \bar{\Psi}m\Psi\right),$$

with the covariant derivative $\mathcal{D}_a = \partial_a - \frac{i}{4}\omega_{bca}\sigma^{bc}$. Here,

$$\omega_{bca} = e_{b\lambda}(\partial_a e_c^{\lambda} + \Gamma^{\lambda}_{\gamma\delta}e_c^{\gamma}e_a^{\delta}),$$

are the spin connections and $\sigma^{bc} = \frac{1}{2}[\gamma^b, \gamma^c]$.

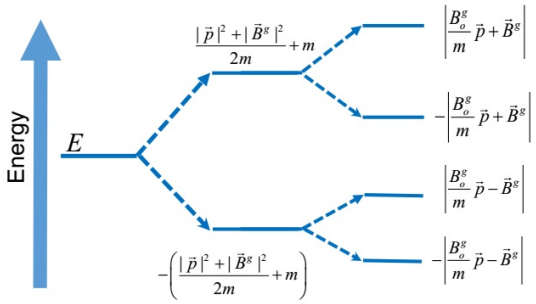

Figure 8.1: Gravitational "Zeeman-splitting": Weak gravitational effect, as given by Eq. (8.3), is considered for the ease of demonstration.

Above equations are written in local inertial frame which is flat along the entire geodesic. Latin and Greek alphabets denote the local flat space and the curved space indices, respectively. e's are the vierbeins connecting curved and locally flat space indices following the relations

$$e^{\delta}_{a}e^{\nu a} = g^{\delta\nu}, \qquad e^{a\delta}e^{b}_{\delta} = \eta^{ab}.$$

Here, η^{ab} and $g^{\delta\nu}$ represent the inertial frame Minkowski metric and curved spacetime metric, respectively.

Hence, Dirac equation in the presence of background gravitational fields, in a local inertial coordinate, reduces as (see, e.g., [84, 233–235])

$$\left[i\gamma^a\partial_a - m + i\gamma^a A^g_a + \gamma^a\gamma^5 B^g_a\right]\psi = 0, \tag{8.1}$$

where A^g_a and B^g_a are the gravitational 4-vector potentials (gravitational coupling with the spinor) and can be given as

$$B^a_g = \epsilon^{abcd}\omega_{bca},$$

m is the mass of spinor, and $\gamma^5 = \gamma_5 = i\gamma^0\gamma^1\gamma^2\gamma^3$ as usual. Here we choose $\hbar = c = 1$. For simplicity, in rest of the discussion, we retain and explore the consequence of the axial-vector-like term only in equation which suffices for the present purpose. This simplification is, however, also consistent in case of Kerr-geometry since the vector-like term is anti-Hermitian for Kerr geometry in local coordinates and can be removed from the total Lagrangian when added to its complex conjugate part. This is particularly so for Majorana neutrinos, when massive neutrinos are most plausibly believed to be Majorana typed. Nevertheless, such a vector-like anti-Hermitian term would not contribute to the effective energy of the particle with an appropriate definition of dot-product in curved spacetime [235, 236].

Now for the nontrivial solution of ψ, the Hamiltonians of the spin-up and spin-down particles are given by

$$(H + \vec{\sigma}.\vec{B^g})^2 = \vec{p}^2 + B^{g2}_0 + m^2 - 2B^g_0\vec{\sigma}.\vec{p}, \tag{8.2}$$

where B^g_0 is the temporal component of B^g_μ. In the regime of weak gravity and when m is much larger than the rest of the terms in the R.H.S. of Eq. (8.2), it reduces to

$$H = -\vec{\sigma}.\vec{B^g} \pm \left[\frac{\vec{p}^2 + B^{g2}_0}{2m} + m - \frac{B^g_0\vec{\sigma}.\vec{p}}{m}\right]. \tag{8.3}$$

There are two-fold splits in dispersion energy, governed by two terms associated with the Pauli spin matrix, between up and down spinors for positive and negative energy solutions. See Fig. 8.1 demonstrating the same. Note that Fig 8.1, based on Eq. (8.3) is given here for a special case of non-relativistic neutrinos to explain the energy splitting for neutrino-antineutrino states of same mass m in a quite simple manner. However, through out the analysis in this chapter we have considered the generalized relativistic case.

In order to have nonzero B^g_a, spherical symmetry has to be broken, hence in Schwarzschild geometry it vanishes. In Schwarzschild metric, any possible effect would arise from A^g_a, which is removed in the present formalism. Indeed it is known [237, 238] that spin evolution in spherical symmetric spacetime could arise only from an imaginary Lorentz vector-like term. On the other hand, in Kerr geometry B^g_a survives. Also it survives in, e.g., early universe under gravity wave perturbation, Bianchi II, VIII and IX anisotropic universes. Note that in an expanding universe, gravitational potential B^g_a turns to be constant at a given epoch which could act as a background effect.

In Kerr-Schild coordinate, after putting $\hbar$ and c appropriately, the temporal part of B^g_a reads as

$$B^g_0 = -\frac{4az}{\bar{\rho}^2\sqrt{2r^3}}\frac{\hbar c}{r_g}, \tag{8.4}$$

where $\bar{\rho}^2 = 2r^2+a^2-x^2-y^2-z^2$, r is the radial coordinate of the system expressed in units of r_g, $r_g = GM/c^2$, M and a (varying from -1 to $+1$) are respectively mass and dimensionless angular momentum per unit mass of the black hole, G, c and $\hbar$ are respectively Newton's gravitation constant, speed of light and reduced Planck's constant. Naturally, B^g_0 survives (and is varying with space coordinates) for any spinning black hole leading to gravitational Zeeman effect.

In Bianchi II spacetime with, e.g., equal scale-factors in all directions, B^g_0 survives as

$$B^g_0 = \frac{4+3y^2-2y}{8+2y^2}\hbar c. \tag{8.5}$$

8.2 Quantum correlations in neutrinos

We will now analyze the neutrino anti-neutrino oscillations in one and two flavour scenarios, which can be viewed as two and four level systems, respectively. The schematic diagram is given in Fig. 8.2.

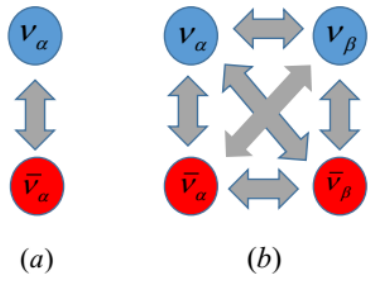

Figure 8.2: Neutrino-antineutrino oscillations in (a) one-flavour, and (b) two-flavour scenarios.

8.2.1 Neutrino-antineutrino mixing in single flavour scenario

Let us consider, in Weyl representation, a 2-level system describing the mixing of neutrino (ψ) and antineutrino (ψ^c) [239] in the presence of gravitational coupling. We can express the states

with known mass (but unknown lepton number states, in the present case spin-states) in terms of states with known lepton/spin-states or vice versa. This is in the spirit of mixing in the neutral kaons, differing by two units of strangeness, whereas for neutrino and antineutrino it differs by two units of lepton number. The corresponding mass eigenstates for a particular flavour at $t = 0$ are [83, 84]

$$\begin{aligned}|\nu_1(0)\rangle &= \cos\theta\,|\psi^c(0)\rangle \;+\; e^{i\phi}\;\sin\theta\,|\psi(0)\rangle\\ |\nu_2(0)\rangle &= -\sin\theta\,|\psi^c(0)\rangle \;+\; e^{i\phi}\;\cos\theta\,|\psi(0)\rangle,\end{aligned} \tag{8.6}$$

when

$$\tan\theta \;=\; \frac{m}{B_0^g + \sqrt{B_0^{g2} + m^2}}, \quad \phi = \arg(-m), \tag{8.7}$$

where m is the Majorana mass of neutrino. Note that the mixing is maximum for $B_0^g = 0$. However, at an arbitrary time t the mass eigenstates are

$$\begin{aligned}|\nu_1(t)\rangle &= \cos\theta\; e^{-iE_{\psi^c}t}\,|\psi^c(0)\rangle \;+\; e^{i\phi}\;\sin\theta\; e^{-iE_{\psi}t}\,|\psi(0)\rangle\\ |\nu_2(t)\rangle &= -\sin\theta\; e^{-iE_{\psi^c}t}\,|\psi^c(0)\rangle \;+\; e^{i\phi}\;\cos\theta\; e^{-iE_{\psi}t}\,|\psi(0)\rangle,\end{aligned} \tag{8.8}$$

where the dispersion energies for neutrino and antineutrino respectively, due to gravitational Zeeman-splitting, from Eq. (8.2) are given by

$$\begin{aligned}E_{\psi} &= \sqrt{(\vec{p} - \vec{B}^g)^2 + m^2} + B_0^g,\\ E_{\psi^c} &= \sqrt{(\vec{p} + \vec{B}^g)^2 + m^2} - B_0^g.\end{aligned} \tag{8.9}$$

For ultra-relativistic neutrinos, $m \ll |\vec{p}|$ leading to $E_{\psi} - E_{\psi^c} \approx 2(B_0^g - |\vec{B}^g|)$, the survival probability of ν_1 at time t can be expressed as

$$\mathcal{P}_s(t) = 1 - \sin^2 2\theta \sin^2\{(B_0^g - |\vec{B}^g|)(t)\}. \tag{8.10}$$

Note that $(\nu_1(0), \nu_2(0))$ is just the transformed spinor of original (ψ^c, ψ). In the limit of zero gravitational effect, i.e., $B_\mu^g \to 0$, $\mathcal{P}_s(t) \to 1$. Thus the neutrino-antineutrino oscillations primarily occur due to non-zero value of the gravitational potential, when the present analysis is performed for ultra-relativistic neutrinos.

In Fig. 8.3(a), the survival probability for $\nu_1 \leftrightarrow \nu_2$ oscillations is shown as a function of gravitational potential and the distance ($L \approx ct$ in ultra relativistic limit[1]) traveled by the neutrino/antineutrino. The survival probability can be seen to approach its maximum value unity as the gravitational potential increases. This implies that gravity suppresses the neutrino-antineutrino oscillations for a *fixed* m. Further, as noted earlier, the neutrino-antineutrino oscillation approaches maximum when $B_0^g \to 0$.

von Neumann entropy in oscillation

The neutrino-antineutrino system can be treated as an effective two qubit system [15, 18, 19, 206] with the following *occupation number* representation of states defined in Eq. (8.6) as

$$|\nu_1(0)\rangle \equiv |10\rangle\,, \qquad |\nu_2(0)\rangle \equiv |01\rangle\,.$$

[1]Here, entire analysis is performed in local inertial coordinates. Hence, at each point, all the special relativistic norms are conveniently satisfied such that at a given local point, B_μ^g appears as constant background field [83].

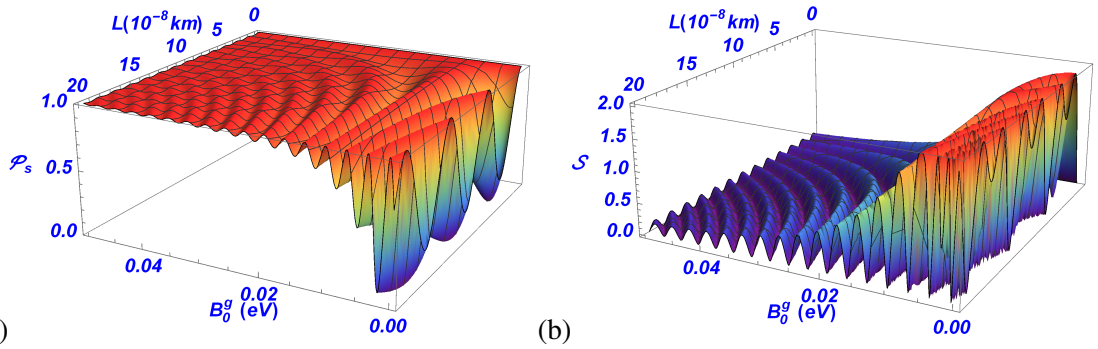

Figure 8.3: Fixed flavour case: (a) Survival probability, and (b) von Neumann entropy, as functions of gravitational potential and distance traveled by neutrino/antineutrino, for the massive states $\nu_1 \leftrightarrow \nu_2$ corresponding to neutrino-antineutrino oscillation. The various parameters used are: $m = 5 \times 10^{-3}$ eV, $|\vec{B^g}| \sim 10^{-2}$ eV.

The notation $|10\rangle$ amounts to asking whether we have a $|\nu_1\rangle$ state or not. In this notation, one can finally write

$$\begin{aligned} |\nu_1(t)\rangle &= \mathcal{U}_{11}(t)\,|10\rangle + \mathcal{U}_{12}(t)\,|01\rangle\,, \\ |\nu_2(t)\rangle &= \mathcal{U}_{21}(t)\,|10\rangle + \mathcal{U}_{22}(t)\,|01\rangle\,, \end{aligned} \tag{8.11}$$

where the coefficients can be obtained from Eqs. (8.6) and (8.8) as

$$\begin{aligned} \mathcal{U}_{11}(t) &= \cos^2\theta e^{-iE_{\psi^c}t} + \sin^2\theta e^{-iE_{\psi}t}, \\ \mathcal{U}_{12}(t) &= \sin\theta\cos\theta(e^{-iE_{\psi}t} - e^{-iE_{\psi^c}t}), \\ \mathcal{U}_{21}(t) &= \sin\theta\cos\theta(e^{-iE_{\psi}t} - e^{-iE_{\psi^c}t}), \\ \mathcal{U}_{22}(t) &= \sin^2\theta e^{-iE_{\psi^c}t} + \cos^2\theta e^{-iE_{\psi}t}. \end{aligned}$$

A standard measure of entanglement for pure states, of form Eq. (8.11), is given by von Neumann entropy

$$\begin{aligned} \mathcal{S} = &- \sum_{\beta=1,2} |\mathcal{U}_{\alpha\beta}(t)|^2 \log_2 |\mathcal{U}_{\alpha\beta}(t)|^2 \\ &- \sum_{\beta=1,2} (1 - |\mathcal{U}_{\alpha\beta}(t)|^2) \log_2 (1 - |\mathcal{U}_{\alpha\beta}(t)|^2). \end{aligned} \tag{8.12}$$

Here $\alpha = 1\ (2)$ corresponds to the ν_1 (ν_2) state. For the $\nu_1 \leftrightarrow \nu_2$ oscillation, Fig. 8.3(b) shows the variation of $\mathcal{S}$ as a function of B_0^g and L. The existence of entanglement is implied by $\mathcal{S} > 0$. The von-Neumann entropy, as an entanglement measure, is suitable for neutrino system since it can be expressed in terms of the survival and transition probabilities, which are experimentally measurable quantities [18]. The increase in the gravitational potential is found to decrease the entanglement in the neutrino-antineutrino system for a *fixed* m. Further, the entropy attains maximum value when the neutrino and antineutrino both survival probabilities and, hence, their transition probabilities are equal.

8.2.2 Two-flavour oscillation with neutrino-antineutrino mixing

In this case, the flavour and mass eigenstates are related via a unitary matrix **V** as follows [83]:

$$\begin{pmatrix} \psi_e^c \\ \psi_\mu^c \\ \psi_e \\ \psi_\mu \end{pmatrix} = \mathbf{V} \begin{pmatrix} \chi_1 \\ \chi_2 \\ \chi_3 \\ \chi_4. \end{pmatrix}, \tag{8.13}$$

where

$$\mathbf{V} = \begin{pmatrix} \cos\theta_e \cos\phi_1 & -\cos\theta_e \sin\phi_1 & -\sin\theta_e \cos\phi_2 & \sin\theta_e \sin\phi_2 \\ \cos\theta_\mu \sin\phi_1 & \cos\theta_\mu \cos\phi_1 & -\sin\theta_\mu \sin\phi_2 & -\sin\theta_\mu \cos\phi_2 \\ \sin\theta_e \cos\phi_1 & -\sin\theta_e \sin\phi_1 & \cos\theta_e \cos\phi_2 & -\cos\theta_e \sin\phi_2 \\ \sin\theta_\mu \sin\phi_1 & \sin\theta_\mu \cos\phi_1 & \cos\theta_\mu \sin\phi_2 & \cos\theta_\mu \cos\phi_2 \end{pmatrix}. \tag{8.14}$$

One should note here that the dimension of the spinor in Eq. (8.13) is now increased as it has 4 components: two of them representing the electron-neutrino (ψ_e) and muon-neutrino (ψ_μ) and remaining two, ψ_e^c and ψ_μ^c, would represent respectively their antiparticles. Consequently, we will also have a spinor $\chi = (\chi_1, \chi_2, \chi_3, \chi_4)^T$ constituting corresponding mass eigenstates, two of them for $\nu_e - \bar{\nu}_e$ mixing and the rest of them for mixing between $\nu_\mu - \bar{\nu}_\mu$. The mixing angles are related to the masses and the gravitational scalar potential as [83]

$$\tan\theta_{e,\mu} = \frac{m_{e,\mu}}{B_0^g + \sqrt{(B_0^g)^2 + m_{e,\mu}^2}}, \tag{8.15}$$

$$\tan\phi_{1,2} = \frac{\mp 2m_{e\mu}}{m_{e(1,2)} - m_{\mu(1,2)} + \sqrt{(m_{e(1,2)} - m_{\mu(1,2)})^2 + 4m_{e\mu}^2}}. \tag{8.16}$$

The masses corresponding to the mass eigenstates are given as

$$\begin{aligned} M_{1,2} &= \frac{1}{2}\left[(m_{e1} + m_{\mu 1}) \pm \sqrt{(m_{e1} - m_{\mu 1})^2 + 4m_{e\mu}^2}\right], \\ M_{3,4} &= \frac{1}{2}\left[(m_{e2} + m_{\mu 2}) \pm \sqrt{(m_{e2} - m_{\mu 2})^2 + 4m_{e\mu}^2}\right], \end{aligned} \tag{8.17}$$

with

$$m_{(e,\mu)1} = -\sqrt{(B_0^g)^2 + m_{e,\mu}^2} \qquad m_{(e,\mu)2} = \sqrt{(B_0^g)^2 + m_{e,\mu}^2}, \tag{8.18}$$

and $m_{e\mu}$ being the mixing mass.

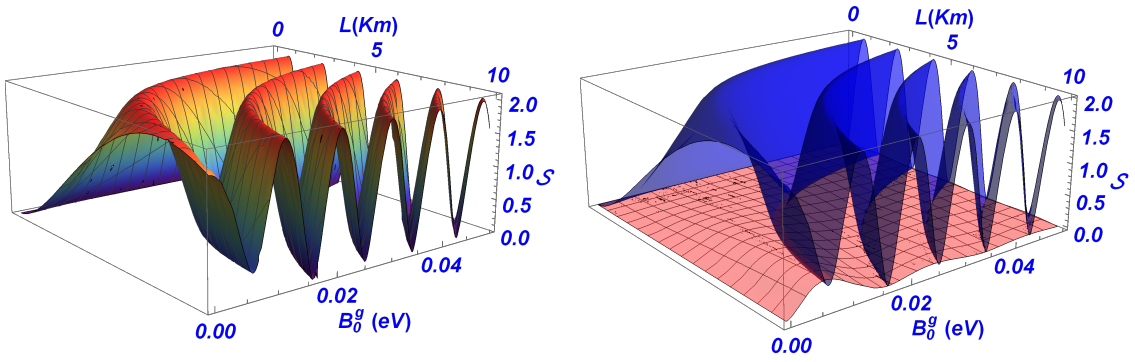

Figure 8.4: Left panel: The variation of von Neumann entropy for 2-flavour neutrino-antineutrino oscillation with respect to the distance (L) traveled by neutrinos and the gravitational potential (B_0^g). Right panel: The contributions to flavour entropy from neutrino-neutrino oscillations depicted by blue (plane) surface and neutrino-antineutrino oscillations shown by pink (meshed) surface, with the magnitude of $\mathcal{S}$ enhanced 10 times in the later case.

Now the system of 2-flavour neutrino oscillations under the influence of neutrino-antineutrino mixing, due to gravitational field, can be treated as a 4-qubit system. The occupation number representation can be given as

$$
\begin{aligned}
|\psi_e^c\rangle &\equiv |1\rangle_{\bar{e}} \otimes |0\rangle_{\bar{\mu}} \otimes |0\rangle_e \otimes |0\rangle_\mu \,, \\
|\psi_\mu^c\rangle &\equiv |0\rangle_{\bar{e}} \otimes |1\rangle_{\bar{\mu}} \otimes |0\rangle_e \otimes |0\rangle_\mu \,, \\
|\psi_e\rangle &\equiv |0\rangle_{\bar{e}} \otimes |0\rangle_{\bar{\mu}} \otimes |1\rangle_e \otimes |0\rangle_\mu \,, \\
|\psi_\mu\rangle &\equiv |0\rangle_{\bar{e}} \otimes |0\rangle_{\bar{\mu}} \otimes |0\rangle_e \otimes |1\rangle_\mu \,.
\end{aligned} \tag{8.19}
$$

Further, Mermin inequality is a generalized form of Bell inequality and its violation indicates the standard nonlocal correlations existing among different parties in a multipartite system [105]. This means that the probability distribution P (say for a tripartite system) cannot be written in the local form

$$
P(a_1 a_2 a_3) = \int d\lambda \rho(\lambda) P_1(a_1|\lambda) P_2(a_2|\lambda) P_3(a_3|\lambda), \tag{8.20}
$$

where λ is the shared local variable and a_1, a_2, a_3 are the outcomes of the measurements. However, this does not ensure the genuine multipartite nonlocality, i.e., if any two subsystems are nonlocally correlated, but uncorrelated from the third one, Mermin inequality can still be violated [209, 210]. To probe genuine nonlocal correlations, we make use of the Svetlichny inequality which is based on hybrid nonlocal-local realism [106] as follows

$$
P_B(a_1 a_2 a_3) = \sum_{k=1}^{3} P_k \int d\lambda \rho_{ij}(\lambda) P_{ij}(a_i a_j|\lambda) P_k(a_k|\lambda). \tag{8.21}
$$

Here the subscript B stands for bipartition sections. For a 4-qubit-system the Mermin (M_4) [240] and Svetlichny (S_4) [241] parameters are defined as

$$
\begin{aligned}
M_4 = &-ABCD + (ABCD' + ABC'D + AB'CD + A'BCD) \\
&+ (ABC'D' + AB'CD' + AB'C'D + A'BCD' + A'BC'D \\
&+ A'B'CD) - (AB'C'D' + A'BC'D' + A'B'CD' \\
&+ A'B'C'D) - A'B'C'D',
\end{aligned} \tag{8.22}
$$

$$
\begin{aligned}
S_4 = &\, ABC'D' + AB'CD' + A'BCD' - A'B'C'D' + \\
&A'B'CD' + A'BC'D' + AB'C'D' - AB'C'D' + A'B'CD \\
&+ A'BC'D + AB'C'D - ABCD + ABC'D + AB'CD + \\
&A'BCD - A'B'C'D.
\end{aligned} \tag{8.23}
$$

Here, X and X' ($X = A, B, C, D$), are two different measurement settings pertaining to each qubit. The classical bounds on these parameters are $M_4 \leq 4$ and $S_4 \leq 8$. It is important to note that for the violation of Mermin inequality, at least one bipartite section must have the nonlocal correlations, while the Svetlichny inequality will be violated only when all the parties are nonlocally correlated.

In Fig. 8.4, the variation of von-Neumann entropy ($\mathcal{S}$) is depicted with respect to the distance L traveled by neutrinos and the gravitational potential B_0^g. In two flavour case the state of the system has four degrees of freedom to oscillate between. With initial state as ν_e, oscillations occur between ν_e, ν_μ, $\bar{\nu}_e$ and $\bar{\nu}_\mu$ flavour modes of the system. Figure 8.4(a) depicts the total flavour entropy with contribution from all the available modes of oscillation, while in Fig. 8.4(b)

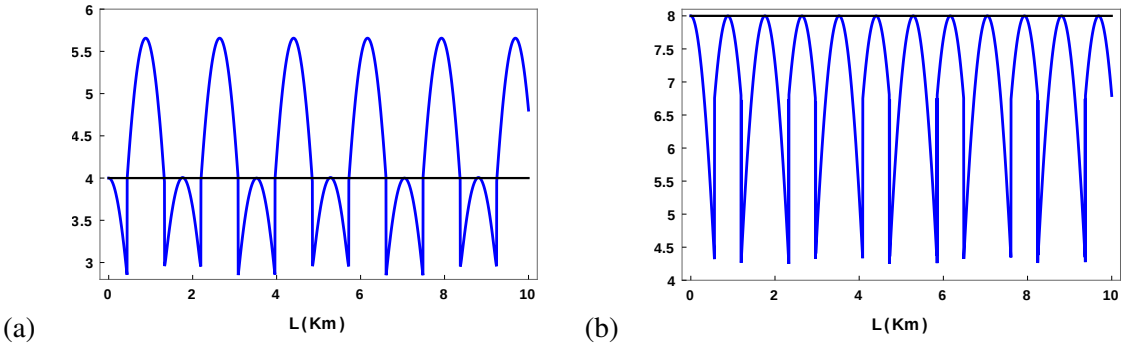

(a) (b)

Figure 8.5: (a) Mermin M_4 and (b) Svetlichny S_4 parameters with respect to the distance (L) traveled by neutrinos with $B_0^g = 5 \times 10^{-2}$. Black lines correspond to the classical bounds of these parameters.

the contribution from particle and antiparticle modes separately is shown. For the sake of clarity, we have enhanced the magnitude of $\mathcal{S}$ by 10 times for antineutrino case. The particle degrees of freedom contribute more to $\mathcal{S}$ in comparison to the antiparticle degrees of freedom. That is, the neutrino-neutrino flavour mixing is dominating over the neutrino-antineutrino mixing. A common feature depicted in Figs. 8.3 and 8.4 is that for neutrino-antineutrino oscillations, $\mathcal{S}$ decreases with the increase in B_0^g. However, for neutrino-neutrino mixing, the increase in B_0^g does not reduce the magnitude of $\mathcal{S}$ but increases the frequency of its oscillation.

Figure 8.5 depicts Mermin and Svetlichny parameters with respect to L, with $B_0^g = 5 \times 10^{-2}$ eV. The violation of the classical bound of M_4 indicates the existence of residual nonlocality in the system. Further, S_4 does not cross the classical bound in our system, thereby showing the absence of genuine nonlocality. This can be attributed to equality of the two mass squared differences, i.e., $\Delta m_{41}^2 = \Delta m_{32}^2 = 0$, suppressing the nonlocal correlations between the degenerate levels $\nu_1 - \nu_4$ and $\nu_2 - \nu_3$.